Efficient and Robust Spectral-Element Methods on Triangles Using Tensor-Product Summation-by-Parts Operators

Advanced Modeling and Simulation (AMS) Seminar Series
NASA Ames Research Center

Tristan Montoya and David W. Zingg

Institute for Aerospace Studies, University of Toronto
4925 Dufferin St, Toronto, ON M3H 5T6, Canada

October 20, 2022

Background

Numerical methods for conservation laws

High-fidelity predictions of **multiscale phenomena** in science and engineering governed by time-dependent **conservation laws** require numerical methods which are:

- **Efficient** – deliver a desired level of accuracy at a reasonable computational cost, scaling effectively to large problem sizes
- **Robust** – consistently provide useful/physically meaningful results for all problems/data within some well defined regime
- **Automated** – achieve the above objectives with minimal user intervention (e.g. parameter tuning or mesh generation)

Scale-resolving simulations of **turbulent flows** largely remain **intractable** in practice using conventional second-order schemes, requiring alternative methods meeting the above requirements

Background

Discontinuous spectral-element methods

Discontinuous **spectral-element methods**[1] on unstructured grids offer:

- **High-order/spectral accuracy** – more accurate than second-order methods for smooth regimes and low error tolerances (for a given number of degrees of freedom)
- **Flexibility** – support for local refinement either by decreasing the element size (h) or increasing the polynomial degree (p)
- **Performance on modern hardware** – compact formulations with high arithmetic intensity

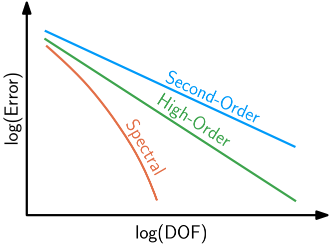

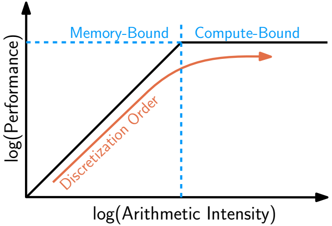

[1] Element-based discretizations achieving high-order accuracy through interior DOF

Background

Tensor-product vs. multidimensional approximations

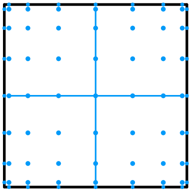

Tensor-product

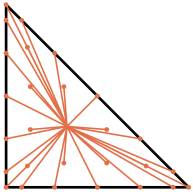

Multidimensional

- Fast matrix-free operator evaluation (i.e. using **sum factorization**[2])
- Typically restricted to quad or hex elements, requires **more user intervention** in body-fitted mesh generation

- **More automated** meshing of complex geometries, facilitates *hp*-adaptation
- **Less efficient** at higher orders due to all-to-all coupling of local degrees of freedom

[2] Introduced in the context of spectral methods by Orszag (1980)

Background

Collapsed coordinate transformation

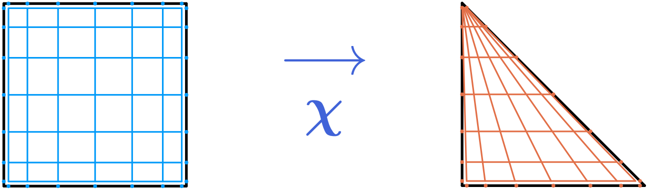

A **collapsed coordinate transformation** (Duffy, 1982) can be used to enable sum factorization on triangles or other domains[3]

Combines the **efficiency** of tensor-product approximations with the **geometric flexibility** of general multidimensional element types

[3] Approach proposed by Dubiner (1991); early applications to **continuous Galerkin** (CG) methods by Sherwin and Karniadakis (1995) and to **discontinuous Galerkin** (DG) schemes by Lomtev and Karniadakis (1999) and Kirby et al. (2000)

Background

Tensor-product spectral-element methods in collapsed coordinates

Collapsed-coordinate approach is now a fairly mature technology, forming the basis for triangular/tetrahedral/prismatic/pyramidal elements in ***Nektar++*** (Cantwell et al., 2015; Moxey et al., 2020)

Results in **efficient algorithms** on modern hardware, for example, with SIMD vectorization (Moxey, Amici, and Kirby, 2020)

However, high-order methods often **lack robustness** when used to solve nonlinear problems or with curvilinear meshes, relying on *ad hoc* techniques to achieve stability in practice, for example:

- Filtering
- Spectral vanishing viscosity (SVV)
- Over-integration

These require parameter tuning, add computational expense, and in the case of filtering/SVV can pollute the solution accuracy

Background

Summation-by-parts property

Modern formulations based on the **summation-by-parts** (SBP) property produce **mathematical guarantees** that numerical schemes will respect certain properties of the partial differential equations they approximate

Exisiting **provably stable high-order methods** for conservation laws on tri/tet elements employ multidimensional SBP operators[4] which require $O(p^{2d})$ operations – much more costly at higher orders than $O(p^{d+1})$ tensor-product schemes on quads or hexes

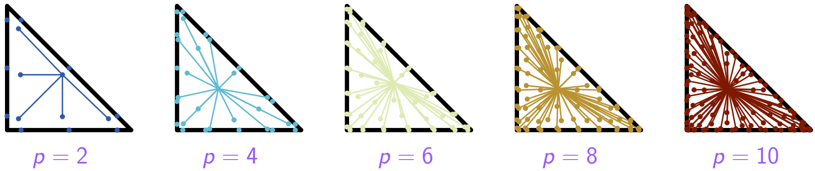

[4]Hicken, Del Rey Fernández, and Zingg, 2016; Chen and Shu, 2017; Del Rey Fernández, Hicken, and Zingg, 2018; Crean et al., 2018; Chan, 2018.

Overview

Research objectives and contributions

Objective: Extend the summation-by-parts framework to spectral-element methods in collapsed coordinates, combining:

- **Efficiency** of arbitary-order tensor-product operators
- **Robustness** of energy-stable/entropy-stable SBP formulations
- **Automation** and geometric flexibility of triangles/tetrahedra

This presentation will focus on discretizations on curved triangular meshes which are **energy stable** for the linear advection equation

The same operators can be used for entropy-stable formulations applied to Euler/Navier-Stokes, and a similar approach can be taken in three dimensions (both are the focus of ongoing work)

Overview

General approach

1. Represent the solution on a canonical reference element $\hat{\Omega} \subset \mathbb{R}^d$ in terms of a **nodal** or **modal** basis supporting sum factorization
2. Construct **tensor-product spectral-element operators in collapsed coordinates** satisfying a discrete analogue of integration by parts for functions $U, V \in C^1(\hat{\Omega})$:

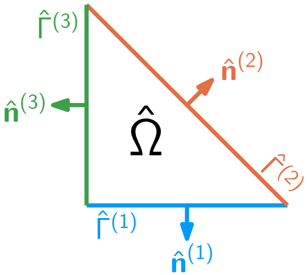

$$\int_{\hat{\Omega}} U \frac{\partial V}{\partial \xi_m} \, d\boldsymbol{\xi} + \int_{\hat{\Omega}} \frac{\partial U}{\partial \xi_m} V \, d\boldsymbol{\xi} = \sum_{\zeta=1}^{N_f} \int_{\hat{\Gamma}^{(\zeta)}} UV \hat{n}_m \, d\hat{s}$$

Overview

General approach

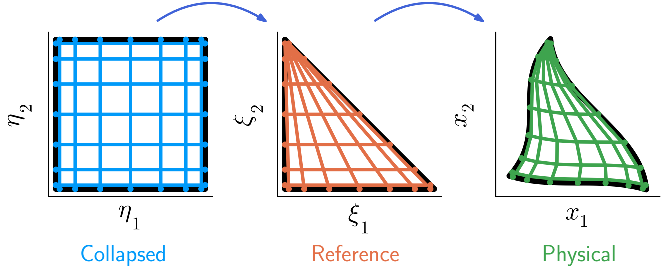

3. Build SBP operators on each physical element from those on the reference element using the **skew-symmetric splitting** proposed by Crean et al. (2018)

4. Recast the action of all physical operators in terms of **one-dimensional operations** along lines of constant η_1 and η_2 to obtain **matrix-free sum-factorization algorithms**

Preliminaries

Gaussian quadrature and Lagrange polynomials in one dimension

Fundamental building blocks of **spectral collocation** methods:

- **Gaussian quadrature rules** with nodes $\{\xi^{(i)}\}_{i\in\{0:q\}}$ and weights $\{\omega^{(i)}\}_{i\in\{0:q\}}$, where $\int_{-1}^{1} V(\xi)\, d\xi \approx \sum_{i=0}^{q} V(\xi^{(i)})\, \omega^{(i)}$ is exact for all $V \in \mathbb{P}_\tau([-1,1])$
- **Lagrange polynomials** $\{\ell^{(i)}\}_{i\in\{0:q\}}$ such that $\ell^{(i)}(\xi^{(j)}) = \delta_{ij}$

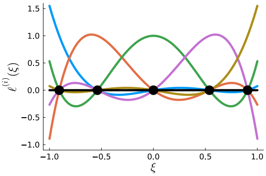

Legendre-Gauss (LG, $\tau = 2q+1$)

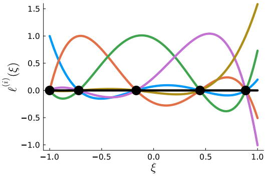

Legendre-Gauss-Radau (LGR, $\tau = 2q$)

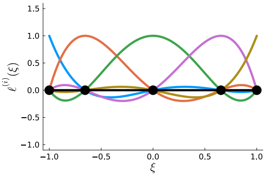

Legendre-Gauss-Lobatto (LGL, $\tau = 2q-1$)

Preliminaries

One-dimensional operations using Lagrange polynomials

Lagrange polynomials enable the following operations on $[-1,1]$:

- **Nodal differentiation** – exact for $V \in \mathbb{P}_q([-1,1])$

$$\begin{bmatrix} \frac{dV}{d\xi}(\xi^{(0)}) \\ \vdots \\ \frac{dV}{d\xi}(\xi^{(q)}) \end{bmatrix} \approx \underbrace{\begin{bmatrix} \frac{d}{d\xi}\ell^{(0)}(\xi^{(0)}) & \cdots & \frac{d}{d\xi}\ell^{(q)}(\xi^{(0)}) \\ \vdots & \ddots & \vdots \\ \frac{d}{d\xi}\ell^{(0)}(\xi^{(q)}) & \cdots & \frac{d}{d\xi}\ell^{(q)}(\xi^{(q)}) \end{bmatrix}}_{=: \underline{\underline{D}}} \begin{bmatrix} V(\xi^{(0)}) \\ \vdots \\ V(\xi^{(q)}) \end{bmatrix}$$

- **Boundary evaluation** – exact at least for $U, V \in \mathbb{P}_q([-1,1])$

$$UV\Big|_{-1}^{1} \approx \begin{bmatrix} U(\xi^{(0)}) \\ \vdots \\ U(\xi^{(q)}) \end{bmatrix}^{\mathsf{T}} \underbrace{\begin{bmatrix} \ell^{(0)}\ell^{(0)}|_{-1}^{1} & \cdots & \ell^{(0)}\ell^{(q)}|_{-1}^{1} \\ \vdots & \ddots & \vdots \\ \ell^{(q)}\ell^{(0)}|_{-1}^{1} & \cdots & \ell^{(q)}\ell^{(q)}|_{-1}^{1} \end{bmatrix}}_{=: \underline{\underline{E}}} \begin{bmatrix} V(\xi^{(0)}) \\ \vdots \\ V(\xi^{(q)}) \end{bmatrix}$$

Preliminaries

One-dimensional SBP property for spectral collocation operators

A stable approximation requires the constituent matrix operators to **satisfy the SBP property** (Kreiss and Scherer, 1974)

$$\begin{array}{ccccc} \displaystyle\int_{-1}^{1} U \frac{dV}{d\xi}\, d\xi & + & \displaystyle\int_{-1}^{1} \frac{dU}{d\xi} V\, d\xi & = & UV\Big|_{-1}^{1} \\ \wr\wr & & \wr\wr & & \wr\wr \\ \underline{u}^{\mathsf{T}} \underline{\underline{M}}\,\underline{\underline{D}}\,\underline{v} & + & \underline{u}^{\mathsf{T}} \underline{\underline{D}}^{\mathsf{T}} \underline{\underline{M}}\,\underline{v} & = & \underline{u}^{\mathsf{T}} \underline{\underline{E}}\,\underline{v}, \end{array}$$

where SPD mass matrix $\underline{\underline{M}}$ defines norm in which stability is proven

Theorem:[5] One-dimensional spectral collocation operators satisfy the SBP property $\underline{\underline{M}}\,\underline{\underline{D}} + \underline{\underline{D}}^{\mathsf{T}} \underline{\underline{M}} = \underline{\underline{E}}$ with diagonal mass matrix $M_{ij} = \omega^{(i-1)} \delta_{ij}$ for positive quadrature rules of degree $\tau \geq 2q - 1$

[5] Carpenter and Gottlieb, 1996; Del Rey Fernández, Boom, and Zingg, 2014

Approximation on the Reference Element

Collapsed coordinate transformation

Any point $\boldsymbol{\eta} \in [-1,1]^2$ can be mapped onto the right-angled triangle $\hat{\Omega} := \{\boldsymbol{\xi} \in [-1,1]^2 : \xi_1 + \xi_2 \leq 0\}$ as $\boldsymbol{\xi} = \boldsymbol{\chi}(\boldsymbol{\eta})$, where

$$\boldsymbol{\chi}(\boldsymbol{\eta}) := \begin{bmatrix} \frac{1}{2}(1+\eta_1)(1-\eta_2) - 1 \\ \eta_2 \end{bmatrix}$$

To integrate on the triangle, we use a change of variables to obtain

$$\int_{\hat{\Omega}} V(\boldsymbol{\xi})\, d\boldsymbol{\xi} = \int_{-1}^{1}\int_{-1}^{1} V(\boldsymbol{\chi}(\boldsymbol{\eta}))\left(\frac{1-\eta_2}{2}\right) d\eta_1 d\eta_2,$$

and, avoiding the singularity $\eta_2 = 1$, the chain rule gives

$$\begin{bmatrix} \frac{\partial}{\partial \xi_1} V(\boldsymbol{\xi}) \\ \frac{\partial}{\partial \xi_2} V(\boldsymbol{\xi}) \end{bmatrix}\Bigg|_{\boldsymbol{\xi}=\boldsymbol{\chi}(\boldsymbol{\eta})} = \frac{2}{1-\eta_2} \begin{bmatrix} 1 & 0 \\ \frac{1}{2}(1+\eta_1) & \frac{1}{2}(1-\eta_2) \end{bmatrix} \begin{bmatrix} \frac{\partial}{\partial \eta_1} V(\boldsymbol{\chi}(\boldsymbol{\eta})) \\ \frac{\partial}{\partial \eta_2} V(\boldsymbol{\chi}(\boldsymbol{\eta})) \end{bmatrix}$$

Approximation on the Reference Element

Nodal and modal bases in collapsed coordinates

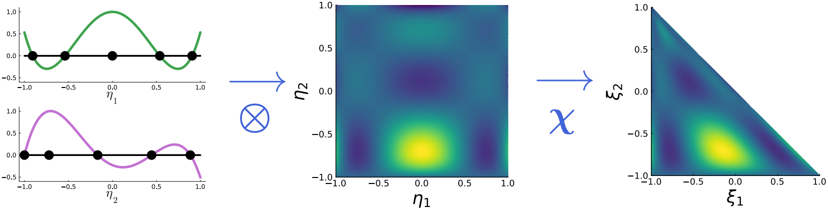

Using the nodal sets $\{\eta_1^{(i)}\}_{i\in\{0:q_1\}}$ and $\{\eta_2^{(i)}\}_{i\in\{0:q_2\}}$, a **nodal basis** can be constructed from one-dimensional Lagrange polynomials as

$$\ell^{(\sigma(\boldsymbol{\alpha}))}(\boldsymbol{\chi}(\boldsymbol{\eta})) := \ell_1^{(\alpha_1)}(\eta_1)\ell_2^{(\alpha_2)}(\eta_2),$$

ordered as $\sigma : \{0 : q_1\} \times \{0 : q_2\} \to \{1 : (q_1 + 1)(q_2 + 1)\}$, where we assume that there is no node at the singularity $\eta_2 = 1$

Approximation on the Reference Element

Nodal and modal bases in collapsed coordinates

Theoretically, the singularity does not pose a significant challenge for the approximation (c.f. Shen, Wang, and Li, 2009) – however, resolution is **concentrated near the singularity**

> *Resolution is a good thing, but this is a case of too much of a good thing because resolution* ***limits the size of explicit time steps*** *(Dubiner, 1991)*

Proriol-Koornwinder-Dubiner (PKD) orthogonal basis for the total-degree p polynomial space $\mathbb{P}_p(\hat{\Omega})$ avoids this issue and has a "warped" tensor-product structure supporting sum factorization:

$$\phi^{(\pi(\boldsymbol{\alpha}))}(\boldsymbol{\chi}(\boldsymbol{\eta})) := \sqrt{2}P_{\alpha_1}^{(0,0)}(\eta_1)(1-\eta_2)^{\alpha_1}P_{\alpha_2}^{(2\alpha_1+1,0)}(\eta_2),$$

where $\pi : \{\boldsymbol{\alpha} \in \mathbb{N}_0^2 : \alpha_1 + \alpha_2 \leq p\} \to \{1 : (p+1)(p+2)/2\}$ and $P_k^{(a,b)}(\eta)$ denotes a normalized Jacobi polynomial of degree k

Approximation on the Reference Element

Nodal and modal bases in collapsed coordinates

We take one of two approaches in this work:

1. **Nodal formulation**
   - Collocate the solution degrees of freedom and fluxes at tensor-product quadrature points in collapsed coordinates, apply operators to nodal values
2. **Modal formulation**
   - Solution degrees of freedom are expansion coefficients for PKD basis (do not correspond to nodal values)
   - Evaluate fluxes at tensor-product quadrature points in collapsed coordinates and apply operators to nodal values

Tensor-product structure of PKD basis permits evaluation at $O(p^d)$ collapsed tensor-product quadrature nodes in $O(p^{d+1})$ operations

Approximation on the Reference Element

Tensor-product summation-by-parts operators on the triangle

Integration must be performed over the **volume** (i.e. interior) and each **facet** (i.e. edge) of the reference triangle:

- **Volume quadrature** – change of variables leads to

$$\boldsymbol{\xi}^{(\sigma(\boldsymbol{\alpha}))} := \boldsymbol{\chi}\big(\eta_1^{(\alpha_1)}, \eta_2^{(\alpha_2)}\big), \quad \omega^{(\sigma(\boldsymbol{\alpha}))} := \omega_1^{(\alpha_1)}\left(\frac{1-\eta_2^{(\alpha_2)}}{2}\omega_2^{(\alpha_2)}\right)$$

- **Facet quadrature** – can align with volume quadrature nodes for more efficient extrapolation from volume to facets

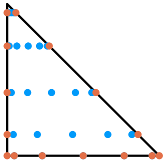

Facet quadrature nodes aligned

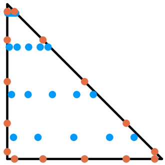

Facet quadrature nodes not aligned

Approximation on the Reference Element

Tensor-product summation-by-parts operators on the triangle

Theorem:[6] Spectral collocation operators on the triangle given by

$$D_{ij}^{(m)} := \frac{\partial \ell^{(j)}}{\partial \xi_m}(\boldsymbol{\xi}^{(i)}), \qquad M_{ij} := \omega^{(i)}\delta_{ij},$$
$$R_{ij}^{(\zeta)} := \ell^{(j)}(\boldsymbol{\xi}^{(\zeta,i)}), \qquad B_{ij}^{(\zeta)} := \omega^{(\zeta,i)}\delta_{ij}$$

are accurate to degree $p = \min(q_1, q_2)$ and satisfy the **SBP property** (Hicken, Del Rey Fernández, and Zingg, 2016)

$$\underline{\underline{M}}\,\underline{\underline{D}}^{(m)} + \left(\underline{\underline{D}}^{(m)}\right)^{\mathsf{T}} \underline{\underline{M}} = \sum_{\zeta=1}^{N_f} \hat{n}_m^{(\zeta)} \left(\underline{\underline{R}}^{(\zeta)}\right)^{\mathsf{T}} \underline{\underline{B}}^{(\zeta)} \underline{\underline{R}}^{(\zeta)},$$

for one-dimensional quadrature rules of at least degree $2q_1$ and $2q_2$ in the η_1 and η_2 directions, respectively

[6] Montoya and Zingg, 2022, Lemma 3.1

Approximation on the Reference Element

Tensor-product summation-by-parts operators on the triangle

Remarks:

- These operators exist for all $p \in \mathbb{N}$ and can be evaluated in $O(p^{d+1})$ operations as opposed to the $O(p^{2d})$ required for non-tensor-product SBP operators (i.e. $\sim p^3$ vs. $\sim p^4$)
- Analysis rules out some choices such as LGL quadrature in η_1 or Jacobi-Gauss(-Radau) quadrature in η_2
- We can use the proposed operators within any numerical framework employing multidimensional SBP operators[7]

[7] Including the entropy-stable schemes reviewed in Chen and Shu (2020)

Extension to Curved Elements

Mapping from reference to physical coordinates

Consider a smooth, time-invariant mapping $\boldsymbol{X}^{(\kappa)} : \hat{\Omega} \to \Omega^{(\kappa)}$, where $\Omega^{(\kappa)} \subset \mathbb{R}^d$ is an element in the mesh $\mathcal{T}^h := \{\Omega^{(\kappa)}\}_{\kappa \in \{1:N_e\}}$

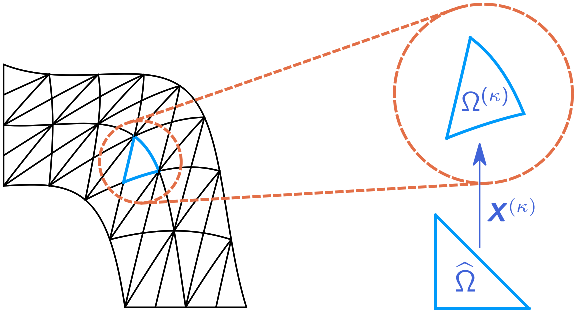

Define $J^{(\kappa)}(\boldsymbol{\xi}) := \det(\nabla_{\boldsymbol{\xi}} \boldsymbol{X}^{(\kappa)}(\boldsymbol{\xi}))$, where $\nabla_{\boldsymbol{\xi}} \boldsymbol{X}^{(\kappa)}(\boldsymbol{\xi}) \in \mathbb{R}^{d \times d}$ is the Jacobian of the mapping, and assume $J^{(\kappa)}(\boldsymbol{\xi}) > 0$ for all $\boldsymbol{\xi} \in \hat{\Omega}$

Extension to Curved Elements

Mapping from reference to physical coordinates

Evaluate geometric terms at volume and facet quadrature nodes as

$$\begin{aligned}
J_{ij}^{(\kappa)} &:= J^{(\kappa)}(\boldsymbol{\xi}^{(i)})\delta_{ij}, \\
J_{ij}^{(\kappa,\zeta)} &:= \| J^{(\kappa)}(\boldsymbol{\xi}^{(\zeta,i)})(\nabla_{\boldsymbol{\xi}} \boldsymbol{X}^{(\kappa)}(\boldsymbol{\xi}^{(\zeta,i)}))^{-\mathsf{T}} \hat{\boldsymbol{n}}^{(\zeta)} \|_2 \delta_{ij}, \\
\Lambda_{ij}^{(\kappa,m,n)} &:= \left[J^{(\kappa)}(\boldsymbol{\xi}^{(i)})(\nabla_{\boldsymbol{\xi}} \boldsymbol{X}^{(\kappa)}(\boldsymbol{\xi}^{(i)}))^{-1} \right]_{mn} \delta_{ij}, \\
N_{ij}^{(\kappa,\zeta,n)} &:= \left[J^{(\kappa)}(\boldsymbol{\xi}^{(\zeta,i)})(\nabla_{\boldsymbol{\xi}} \boldsymbol{X}^{(\kappa)}(\boldsymbol{\xi}^{(\zeta,i)}))^{-\mathsf{T}} \hat{\boldsymbol{n}}^{(\zeta)} \right]_{n} \delta_{ij}
\end{aligned}$$

In two dimensions, the **discrete metric identities**/geometric conservation law (Thomas and Lombard, 1979) are **satisfied automatically**[8] if $\boldsymbol{X}^{(\kappa)}$ is a polynomial of degree $p_{\mathrm{map}} \leq p + 1$

Mapping in this work uses **Lagrange polynomials** on symmetric nodal sets (only need multidimensional operators in preprocessing)

[8] Otherwise, the exact metrics must be replaced by approximations such as those of Kopriva (2006) or Crean et al. (2018)

Extension to Curved Elements

Summation-by-parts operators on mapped elements

Skew-symmetric formulation from Crean et al. (2018) results in

$$\underline{\underline{Q}}^{(\kappa,n)} := \frac{1}{2}\sum_{m=1}^{d}\Big(\underline{\underline{\Lambda}}^{(\kappa,m,n)}\underline{\underline{M}}\,\underline{\underline{D}}^{(m)} - \big(\underline{\underline{D}}^{(m)}\big)^{\mathsf{T}}\underline{\underline{M}}\,\underline{\underline{\Lambda}}^{(\kappa,m,n)}\Big) + \frac{1}{2}\sum_{\zeta=1}^{N_f}\big(\underline{\underline{R}}^{(\zeta)}\big)^{\mathsf{T}}\underline{\underline{B}}^{(\zeta)}\underline{\underline{N}}^{(\kappa,\zeta,n)}\underline{\underline{R}}^{(\zeta)}$$

Theorem:[9] Derivative operator $\underline{\underline{D}}^{(\kappa,\zeta)} := (\underline{\underline{M}}\,\underline{\underline{J}}^{(\kappa)})^{-1}\underline{\underline{Q}}^{(\kappa,\zeta)}$ is an approximation of order $p = \min(q_1, q_2)$ to $\partial/\partial x_n$ and satisfies the SBP property on the **physical element** as

$$\underline{\underline{Q}}^{(\kappa,n)} + \big(\underline{\underline{Q}}^{(\kappa,n)}\big)^{\mathsf{T}} = \sum_{\zeta=1}^{N_f}\big(\underline{\underline{R}}^{(\zeta)}\big)^{\mathsf{T}}\underline{\underline{B}}^{(\zeta)}\underline{\underline{N}}^{(\kappa,\zeta,n)}\underline{\underline{R}}^{(\zeta)}$$

[9] Adapted from Crean et al. (2018, Theorem 5)

Putting It All Together

Discontinuous Galerkin formulation

Integrate conservation law $\partial_t U + \nabla_{\boldsymbol{x}} \cdot \boldsymbol{F}(U) = 0$ by parts on $\Omega^{(\kappa)} \in \mathcal{T}^h$ against a test function V and insert numerical flux F^*:

$$\int_{\Omega^{(\kappa)}} \left(V \frac{\partial U}{\partial t} - \nabla_{\boldsymbol{x}} V \cdot \boldsymbol{F}(U) \right) d\boldsymbol{x} + \int_{\partial\Omega^{(\kappa)}} V F^*(U, U^+, \boldsymbol{n})\, ds = 0$$

- **Nodal formulation** – Evaluate flux components at volume quadrature nodes $\underline{f}^{(h,\kappa,n)}(t)$ in terms of nodal coefficients $\underline{u}^{(h,\kappa)}(t)$ and use $\underline{\underline{R}}^{(\zeta)} \underline{u}^{(h,\kappa)}(t)$ from interior and exterior states to obtain numerical flux at facet quadrature nodes $\underline{f}^{(*,\kappa,\zeta)}(t)$
- **Modal formulation** – Compute nodal values in terms of modal coefficients $\underline{\tilde{u}}^{(h,\kappa)}(t)$ as $\underline{u}^{(h,\kappa)}(t) = \underline{\underline{V}}\, \underline{\tilde{u}}^{(h,\kappa)}(t)$, where $V_{ij} = \phi^{(j)}(\boldsymbol{\xi}^{(i)})$, then compute $\underline{f}^{(h,\kappa,n)}(t)$ and $\underline{f}^{(*,\kappa,\zeta)}(t)$

Putting It All Together

Algebraic discretization using SBP operators

Encapsulating the skew-symmetric splitting within the weak-form stiffness operator $\left(\underline{\underline{Q}}^{(\kappa,n)}\right)^{\mathsf{T}}$, we obtain the **nodal formulation**

$$\underline{\underline{M}}\,\underline{\underline{J}}^{(\kappa)}\frac{d\underline{u}^{(h,\kappa)}(t)}{dt} - \sum_{n=1}^{d}\left(\underline{\underline{Q}}^{(\kappa,n)}\right)^{\mathsf{T}}\underline{f}^{(h,\kappa,n)}(t) + \sum_{\zeta=1}^{N_f}\left(\underline{\underline{R}}^{(\zeta)}\right)^{\mathsf{T}}\underline{\underline{B}}^{(\zeta)}\underline{\underline{J}}^{(\kappa,\zeta)}\underline{f}^{(*,\kappa,\zeta)}(t) = \underline{0}$$

and the **modal formulation**

$$\underline{\underline{V}}^{\mathsf{T}}\underline{\underline{M}}\,\underline{\underline{J}}^{(\kappa)}\underline{\underline{V}}\frac{d\underline{\tilde{u}}^{(h,\kappa)}(t)}{dt} - \underline{\underline{V}}^{\mathsf{T}}\left(\sum_{n=1}^{d}\left(\underline{\underline{Q}}^{(\kappa,n)}\right)^{\mathsf{T}}\underline{f}^{(h,\kappa,n)}(t) + \sum_{\zeta=1}^{N_f}\left(\underline{\underline{R}}^{(\zeta)}\right)^{\mathsf{T}}\underline{\underline{B}}^{(\zeta)}\underline{\underline{J}}^{(\kappa,\zeta)}\underline{f}^{(*,\kappa,\zeta)}(t)\right) = \underline{0}$$

Putting It All Together

Theoretical analysis

Theorem:[10] The proposed nodal and modal schemes are:

- Element-wise and globally conservative
- Free-stream preserving (i.e. $\frac{d}{dt}\underline{u}^{(h,\kappa)}(t) = 0$ for constant state)
- Energy conservative (resp. dissipative) for the linear advection equation $\partial_t U + \nabla_{\boldsymbol{x}} \cdot (\boldsymbol{a} U) = 0$ when used with a central (resp. upwind) numerical flux

For **periodic advection problems**, we have:

$$\frac{d}{dt}\left(\sum_{\kappa=1}^{N_e} \underline{1}^{\mathsf{T}} \underline{\underline{M}}\,\underline{\underline{J}}^{(\kappa)} \underline{u}^{(h,\kappa)}(t)\right) = 0$$

$$\frac{d}{dt}\left(\sum_{\kappa=1}^{N_e} \frac{1}{2}\left(\underline{u}^{(h,\kappa)}(t)\right)^{\mathsf{T}} \underline{\underline{M}}\,\underline{\underline{J}}^{(\kappa)} \underline{u}^{(h,\kappa)}(t)\right) \leq 0$$

[10] See Montoya and Zingg, 2022, Theorems 4.1 – 4.3, for precise statement/proofs

Putting It All Together

Efficient implementation

Implementation in **Julia** code `CLOUD.jl`[11] applies physical operators such as $\left(\underline{\underline{Q}}^{(\kappa,n)}\right)^{\mathsf{T}}$ and $\left(\underline{\underline{R}}^{(\zeta)}\right)^{\mathsf{T}}\underline{\underline{B}}^{(\zeta)}\underline{\underline{J}}^{(\kappa,\zeta)}$ using **lazy evaluation** – action on a vector computed using a **strategy dispatched at runtime:**

- **Reference operator** – evaluate action of physical operators using matrices such as $\underline{\underline{D}}^{(m)}$ and $\underline{\underline{R}}^{(\zeta)}$ formed in preprocessing
- **Physical operator** – explicitly form physical operator matrices in preprocessing step and store for each element
- **Tensor product** – Evaluate physical operators in terms of one-dimensional operators (applicable only to collapsed formulations and standard quad/hex schemes)

[11] Conservation Laws on Unstructured Domains – available at https://github.com/tristanmontoya/CLOUD.jl

Putting It All Together

Operator evaluation strategies for $(\underline{\underline{Q}}^{(\kappa,n)})^{\mathsf{T}}$

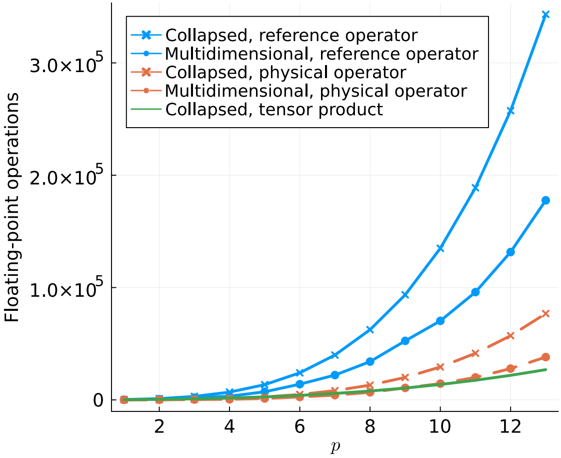

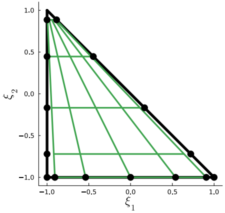

Collapsed

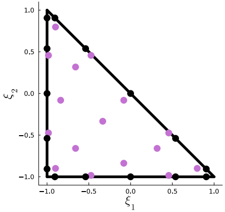

Multidimensional

Putting It All Together

Operator evaluation strategies for $(\underline{\underline{R}}^{(\zeta)})^{\mathsf{T}}\underline{\underline{B}}^{(\zeta)}\underline{\underline{J}}^{(\kappa,\zeta)}$

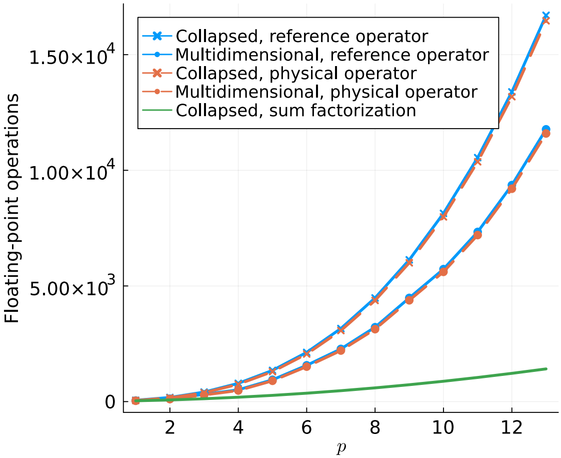

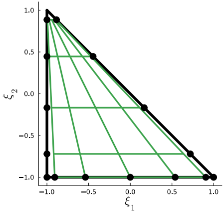

Collapsed

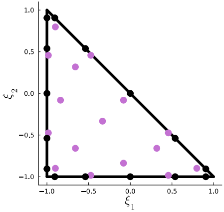

Multidimensional

Numerical Experiments

Problem setup and mesh

Solve the **linear advection equation** with a constant wave speed of $\boldsymbol{a} := [1, 1]^{\mathsf{T}}$ on a periodic square domain $\Omega := (0, 1)^2$

Warp a uniform mesh with N_e elements using Lagrange basis of degree p to mimic high-order meshing of complex geometries

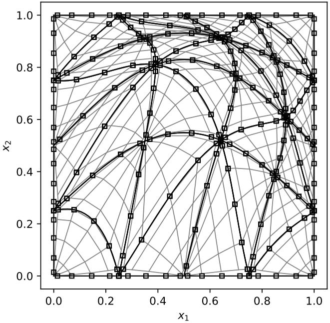

Example mesh for $p = 4$ and $N_e = 32$

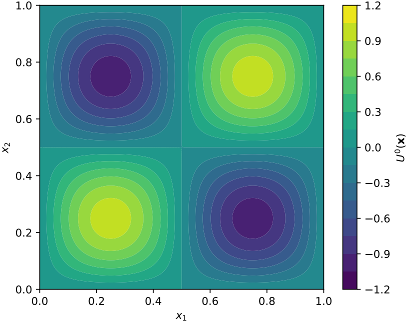

Sinusoidal initial condition

Numerical Experiments

Semi-discrete operator spectra for $p = 4$ and $N_e = 32$

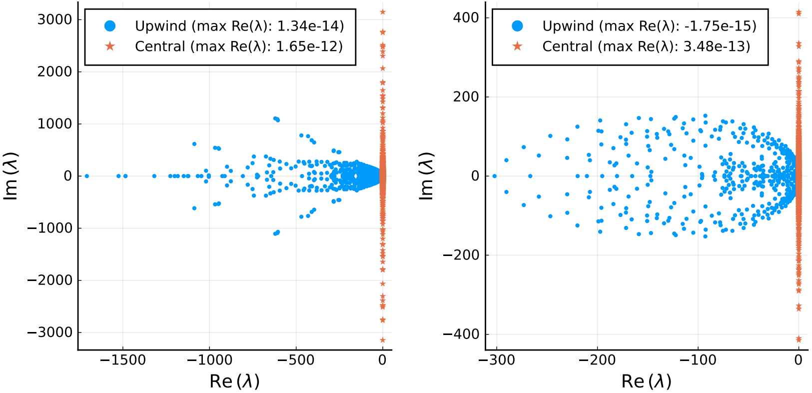

Nodal formulation

Modal formulation

Numerical Experiments

Grid refinement studies (reference 5th and 10th order slopes pictured)

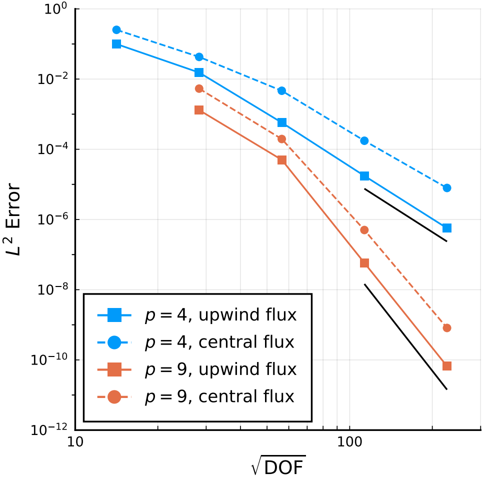

Nodal formulation

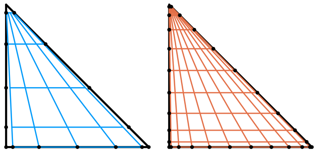

$p = 4$ $\quad$ $p = 9$

- ✓ Conservative
- ✓ Energy dissipative for upwind flux
- ✓ Energy conservative for central flux

Numerical Experiments

Grid refinement studies (reference 5th and 10th order slopes pictured)

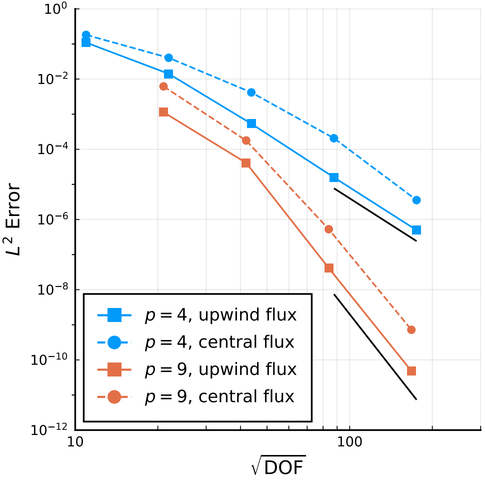

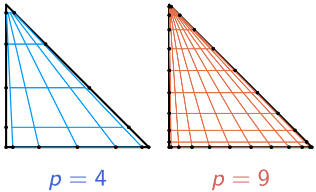

✓ Conservative

✓ Energy dissipative for upwind flux

✓ Energy conservative for central flux

Modal formulation

Numerical Experiments

Grid refinement studies (reference 5th and 10th order slopes pictured)

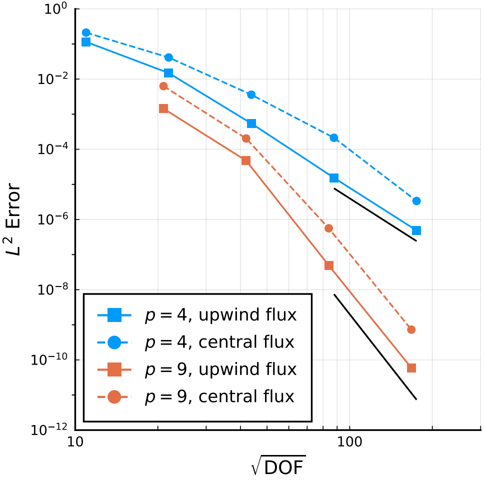

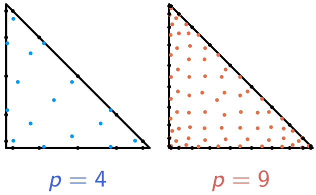

- ✓ Conservative
- ✓ Energy dissipative for upwind flux
- ✗ Energy conservative for central flux

Standard DG (weak conservation form)

Conclusions

By **extending the SBP approach to tensor-product discretizations in collapsed coordinates**, we have laid the theoretical groundwork for robust schemes suitable for complex geometries which extend efficiently to arbitrary order

Presented **nodal formulation** (diagonal mass matrix in curvilinear coordinates, solution directly available at quadrature nodes) and **modal formulation** (minimal DOF, allows for larger time steps)

Future work includes three-dimensional problems, entropy-stable discretizations of nonlinear conservation laws

https://tjbmontoya.com/ https://github.com/tristanmontoya/CLOUD.jl
tristan.montoya@mail.utoronto.ca

Questions?

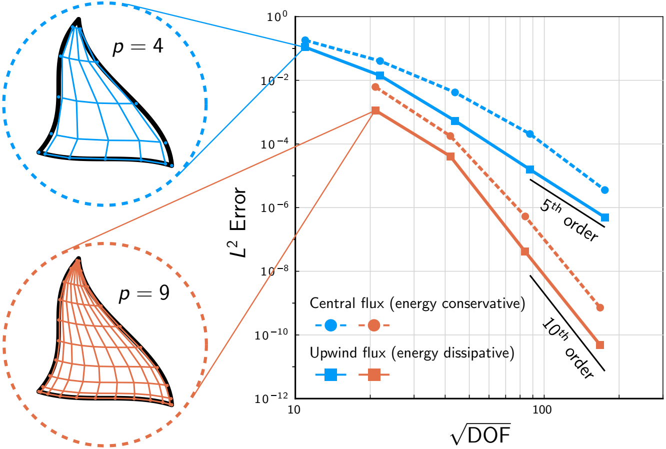

Grid refinement studies: skew-symmetric modal formulation for the linear advection equation

UNIVERSITY OF TORONTO

Alliance de recherche numérique du Canada | Digital Research Alliance of Canada

SciNet

Ontario

References I

Cantwell, C. D. et al. (July 2015). "Nektar++: An open-source spectral/hp element framework." *Computer Physics Communications* 192, pp. 205–219.

Carpenter, Mark H. and David Gottlieb (Nov. 1996). "Spectral Methods on Arbitrary Grids." *Journal of Computational Physics* 129, pp. 74–86.

Chan, Jesse (June 2018). "On Discretely Entropy Conservative and Entropy Stable Discontinuous Galerkin Methods." *Journal of Computational Physics* 362, pp. 346–374.

Chen, Tianheng and Chi-Wang Shu (Sept. 2017). "Entropy Stable High Order Discontinuous Galerkin Methods with Suitable Quadrature Rules for Hyperbolic Conservation Laws." *Journal of Computational Physics* 345, pp. 427–461.

— (June 2020). "Review of Entropy Stable Discontinuous Galerkin Methods for Systems of Conservation Laws on Unstructured Simplex Meshes." *CSIAM Transactions on Applied Mathematics* 1.1, pp. 1–52.

References II

- Crean, Jared et al. (Mar. 2018). "Entropy-Stable Summation-by-Parts Discretization of the Euler Equations on General Curved Elements." *Journal of Computational Physics* 356, pp. 410–438.
- Del Rey Fernández, David C., Pieter D. Boom, and David W. Zingg (June 2014). "A Generalized Framework for Nodal First Derivative Summation-by-Parts Operators." *Journal of Computational Physics* 266, pp. 214–239.
- Del Rey Fernández, David C., Jason E. Hicken, and David W. Zingg (Apr. 2018). "Simultaneous Approximation Terms for Multi-dimensional Summation-by-Parts Operators." *Journal of Scientific Computing* 75.1, pp. 83–110.
- Dubiner, Moshe (Dec. 1991). "Spectral Methods on Triangles and Other Domains." *Journal of Scientific Computing* 6.4, pp. 345–390.

References III

Duffy, Michael G. (Dec. 1982). “Quadrature Over a Pyramid or Cube of Integrands with a Singularity at a Vertex.” *SIAM Journal on Numerical Analysis* 19.6, pp. 1260–1262.

Hicken, Jason E., David C. Del Rey Fernández, and David W. Zingg (July 2016). “Multidimensional Summation-by-Parts Operators: General Theory and Application to Simplex Elements.” *SIAM Journal on Scientific Computing* 38.4, A1935–A1958.

Kirby, Robert M. et al. (May 2000). “A Discontinuous Galerkin Spectral/*hp* Method on Hybrid grids.” *Applied Numerical Mathematics* 33.1-4, pp. 393–405.

Kopriva, David A. (Mar. 2006). “Metric Identities and the Discontinuous Spectral Element Method on Curvilinear Meshes.” *Journal of Scientific Computing* 26.3, pp. 301–327.

References IV

Kreiss, Heinz-Otto and Godela Scherer (1974). "Finite Element and Finite Difference Methods for Hyperbolic Partial Differential Equations." *Mathematical Aspects of Finite Elements in Partial Differential Equations*. Ed. by Carl de Boor. Academic Press, pp. 195–212.

Lomtev, Igor and George Em Karniadakis (Mar. 1999). "A discontinuous Galerkin method for the Navier–Stokes equations." *International Journal for Numerical Methods in Fluids* 29.5, pp. 587–603.

Montoya, Tristan and David W Zingg (July 2022). "Stable and Conservative High-Order Methods on Triangular Elements Using Tensor-Product Summation-by-Parts Operators." *Eleventh International Conference on Computational Fluid Dynamics*.

References V

Moxey, David, Roman Amici, and Robert M. Kirby (May 2020). "Efficient Matrix-Free High-Order Finite Element Evaluation for Simplicial Elements." *SIAM Journal on Scientific Computing* 42.3, pp. C97–C123.

Moxey, David et al. (Apr. 2020). "Nektar++: Enhancing the capability and application of high-fidelity spectral/hp element methods." *Computer Physics Communications* 249, p. 107110.

Orszag, Steven A (Aug. 1980). "Spectral Methods for Problems in Complex Geometries." *Journal of Computational Physics* 37.1, pp. 70–92.

Shen, Jie, Li-Lian Wang, and Huiyuan Li (Jan. 2009). "A Triangular Spectral Element Method Using Fully Tensorial Rational Basis Functions." *SIAM Journal on Numerical Analysis* 47.3, pp. 1619–1650.

References VI

Sherwin, Spencer J. and George E. Karniadakis (June 1995). "A Triangular Spectral Element Method: Applications to the Incompressible Navier-Stokes Equations." *Computer Methods in Applied Mechanics and Engineering* 123.1-4, pp. 189–229.

Thomas, P. D. and C. K. Lombard (Oct. 1979). "Geometric Conservation Law and Its Application to Flow Computations on Moving Grids." *AIAA Journal* 17.10, pp. 1030–1037.